Available online at www.sciencedirect.com

SCIENCE DIRECT®

Solid State Ionics 175 (2004) 797–803

SOLID STATE IONICS

www.elsevier.com/locate/ssi

Pt-based anode catalysts for direct ethanol fuel cells

W.J. Zhou[a], S.Q. Song[a], W.Z. Li[a], G.Q. Sun[a], Q. Xin[a,*], S. Kontou[b], K. Poulianitis[b], P. Tsiakaras[b,*]

[a]*Dalian Institute of Chemical Physics, China Academy of Science, P.O. Box 110, Dalian 116023, P.R. China*
[b]*Department of Mechanical and Industrial Engineering, School of Engineering, University of Thessalia, Pedion Areos, 383 34 Volos, Greece*

Received 20 August 2004; received in revised form 2 September 2004; accepted 7 September 2004

Abstract

In the present work, several carbon supported PtSn and PtSnRu catalysts were prepared with different atomic ratios and tested in direct ethanol fuel cells (DEFC) operated at lower temperature (T=90 °C). XRD and TEM results indicate that all of these catalysts consist of uniform nano-sized particles of narrow distribution and the average particle sizes are always less than 3.0 nm. As the content of Sn increases, the Pt lattice parameter becomes longer. Single direct ethanol fuel cell tests were used to evaluate the performance of carbon supported PtSn catalysts for ethanol electro-oxidation. It was found that the addition of Sn can enhance the activity towards ethanol electro-oxidation. It is also found that a single DEFC of Pt/Sn atomic ratio≤2, "Pt_1Sn_1/C, Pt_3Sn_2/C, and Pt_2Sn_1/C'' shows better performance than those with Pt_3Sn_1/C and Pt_4Sn_1/C. But even adopting the least active PtSn catalyst, Pt_4Sn_1/C, the DEFC also exhibits higher performance than that with the commercial Pt_1Ru_1/C, which is dominatingly used in PEMFC at present as anode catalyst for both methanol electro-oxidation and CO-tolerance. At 90 °C, the DEFC exhibits the best performance when Pt_2Sn_1/C is adopted as anode catalysts. This distinct difference in DEFC performance between the catalysts examined here is attributed to the so-called bifunctional mechanism and to the electronic interaction between Pt and Sn. It is thought that $-OH_{ads}$, surface Pt active sites and the ohmic effect of PtSn/C catalyst determines the electro-oxidation activity of PtSn catalysts with different Pt/Sn ratios.

Keywords: Direct ethanol fuel cells (DEFCs); Carbon supported PtSn catalysts; Polymer exchange electrolyte

1. Introduction

Polymer exchange electrolyte fuel cells (PEMFCs) fed directly by liquid fuels and operated at lower temperature are gaining more attention in the recent years and offer a promise as devices for traction applications because they allow easy handling and storing of the liquid fuel. Operation on liquid fuel can greatly simplify the fuel cell system as well as reduce the infrastructure needed to supply fuel to passenger cars and commercial fleets, assisting in rapid commercialization of fuel cell technology. This type of fuel cells are also promising candidates for portable power sources and stationary applications because they discard bulky fuel processing equipment. Low-molecular weight alcohols such as ethanol and methanol are reasonably inexpensive, nontoxic and largely available and have higher electrochemical reactivity at relatively low temperatures. At present, direct methanol fuel cells (DMFCs) are actively investigated and thought as a possible alternative to H_2/air PEMFCs, and great progress has been made in this field recently [1,2]. Although methanol is the simplest alcohol and is viewed as a good fuel for low-temperature fuel cells, it is still desirable to increase the number of liquid fuels for employment in these fuel cell systems in order to extend their practical applications and to facilitate their commerci-

* Corresponding authors. Qin Xin is to be contacted at Dalian Institute of Chemical Physics, China Academy of Science, P.O. Box 110, Dalian 116023, China, P.R. Tel./fax: +86 411 4379710. Tsiakaras Panagiotis, Department of Mechanical and Industrial Engineering, School of Engineering, University of Thessalia, Pedion Areos, 383 34 Volos, Greece. Tel.: +30 24210 74065.

E-mail addresses: xinqin@dicp.ac.cn (Q. Xin), tsiak@mie.uth.gr (P. Tsiakaras).

0167-2738/$ - see front matter © 2004 Elsevier B.V. All rights reserved.
doi:10.1016/j.ssi.2004.09.055

alization. Besides methanol, other low-weight molecular chemicals such as formic acid [3], ethanol and propanol [4] are also good fuels for low-temperature fuel cells. Among them, ethanol is safer and more convenient, having more energy density (8.01 vs. 6.09 kW h kg^{-1}) than methanol, and appears to fulfill most of fuel requirements for low temperature fuel cells. Furthermore, ethanol has a similar molecular structure to methanol and is the most simplest chain alcohol. In particular, ethanol is a green fuel and can be easily produced in great quantity through fermentation of sugar-containing raw materials and from biomasses. The theoretical open circuit potential (OCP) for ethanol-oxygen fuel cell, as calculated from the Gibbs-free energy, is 1.145 V [5], lower than that of methanol-oxygen fuel cell. The energy efficiency of ethanol-oxygen fuel cell under reversible conditions is similar to that of methanol-oxygen fuel cell, and both are much better than that of a H_2/O_2 fuel cell. Therefore, ethanol is a very attractive fuel for low-temperature fuel cells.

The adsorption and oxidation of ethanol have been thoroughly investigated for over 20 years, but it is still difficult to exactly elucidate its anodic oxidation reaction mechanism. The complete electro-oxidation of ethanol involves 12 electrons per molecule and three water molecules, as follows:

$$CH_3CH_2OH + 3H_2O \rightarrow 2CO_2 + 12H^+ + 12e^-$$

Ethanol electro-oxidation to carbon dioxide also requires the cleavage of the C−C bond, which is different from that of methanol. The cleavage of the C−C bond plays a key role in the ethanol electro-oxidation and determines the fuel efficiency and electrical energy yield. It is reported that at higher temperature, the electrochemical reactivity of ethanol on Pt-based catalyst is not significantly lower than methanol [6], but their reactivities differ greatly at low temperature. It is estimated from the detailed analysis of reaction products that the electro-oxidation of ethanol involves parallel and consecutive oxidation reaction [5,7,8]. Methanol electro-oxidation has been thoroughly investigated over several decades, so that not only the reaction mechanism but also the suitable anode catalysts are now well established and identified. But at present, it is still difficult to identify the appropriate anode catalysts for ethanol electro-oxidation. Besides Pt, other metals such as gold, rhodium and palladium have been investigated as anode catalysts for ethanol electro-oxidation and show a certain activities, but it is found from the previous literature that only platinum is the best catalyst for ethanol electro-oxidation from a practical point of view, particularly in acid medium, where platinum is the only active and stable noble metal. The nature and the structure of the electrode material affect the adsorption and electro-oxidation of ethanol, controlling the formation of adsorbed intermediates and the products. In order to accelerate the development of DEFCs, it is necessary to develop highly active anode catalysts for ethanol electro-oxidation. In this present work, a novel preparation method was used to synthesize several carbon supported PtSn catalysts with different Pt/Sn atomic ratio. The physicochemical characterizations of these catalysts were carried out by transmission electron microscopy (TEM) and X-ray power diffraction (XRD). Single direct ethanol fuel cell (DEFC) tests were operated at different temperature and used to evaluate the activities for ethanol electro-oxidation.

2. Experimental

All carbon XC-72R supported PtSn and PtSnRu catalysts were synthesized according to literature [9]. All catalysts were marked as $Pt_xSn(Ru)_y/C$ or $Pt_xSn_yRu_z/C$ and the subscript denoted atomic ratio of Pt to Sn (or Ru). The Pt loading was 20 wt.% identically in every catalyst sample. The XRD was carried out on Rigaku X-3000 X-ray powder diffractometer scanning from 20° to 90° with a scan rate of 4°/min. A second fine scan with a scan rate of 1°/min from 60° to 75° was carried out to obtain the Pt (220) reflection peaks, and the (220) peak was fitted using the Gaussian function in order to calculate the particle size and lattice parameters [10]. Catalyst samples were examined using the JEOL JEM-2011 electron microscope operated at 100 kV. More than 300 particles were calculated to obtain the integrated information of every catalyst. The membrane electrode assembles (MEAs), in which cathode contained commercial Pt/C catalyst (20 wt.%) with a metal loading of 1.0 mg Pt/cm^2, were manufactured by pressing the electrodes onto both sides of Nafion®-115 membrane at 130 °C for 90 s. The anode contained the different carbon-supported PtSn catalysts with a Pt loading of 1.33 mg/cm^2 (when Pt/C was used as anode catalyst, the metal loading in catalyst layer was 2.0 mg/cm^2). The MEA was loaded into an in-house single-cell test fixture and aqueous solutions of ethanol and unhumidified oxygen with 2 atm(abs) backpressure were directly fed to anode and cathode, respectively. Other operation conditions for the direct ethanol fuel cells were 1.0 ml/min of 1 M ethanol concentration without backpressure at anode side, and the operation temperature was 90 °C.

3. Results and discussion

3.1. XRD and TEM results

XRD patterns of all Pt-based catalyst samples in Figs. 1 and 2 clearly demonstrate the characteristic peak of the Pt fcc structure. In Fig. 1A, no obvious peaks for Sn and its oxides are shown. As observed in Fig. 2, there are also no obvious peaks for Sn and hcp Ru metals or their oxides/hydroxides. The 2θ of the (220) peak for PtSn/C with different atomic ratios, which have angle shifts lower than

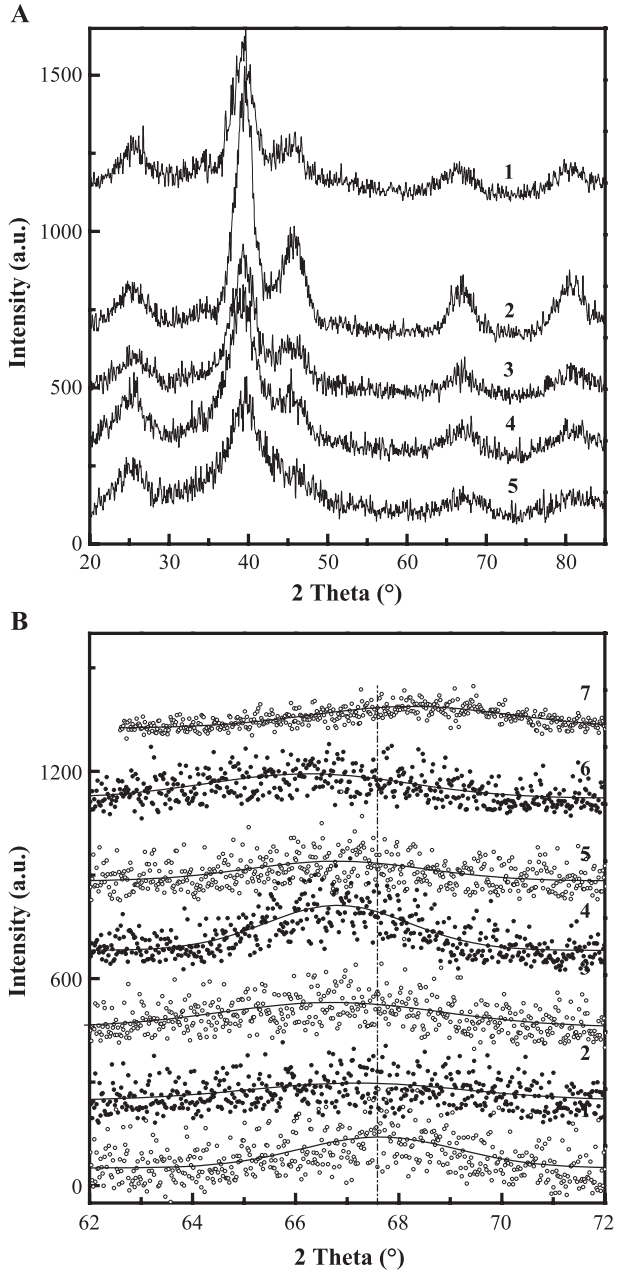

Fig. 1. (A) XRD of carbon supported PtSn with different atomic ratio 1: Pt_1Sn_1/C; 2: Pt_2Sn_1/C; 3: Pt_3Sn_2/C; 4: Pt_3Sn_1/C; 5: Pt_4Sn_1/C. (B) XRD of carbon supported PtSn with different atomic ratio 1: Pt/C; 2: Pt_4Sn_1/C; 3: Pt_3Sn_1/C; 4: Pt_2Sn_1/C; 5: Pt_3Sn_2/C; 6: Pt_1Sn_1/C; 7: Pt_1Ru_1/C.

67.62 of Pt/C and 68.26 of Pt_1Ru_1/C synthesized by the same method, are 67.17 (Pt_4Sn_1/C), 66.89 (Pt_3Sn_1/C), 66.82 (Pt_2Sn_1/C), 66.50 (Pt_3Sn_2/C) and 66.24 (Pt_1Sn_1/C), respectively, as seen in Fig. 1B. The lower angle shifts of the Pt peaks account for the alloy formation and the interaction between Pt and Sn. By fitting the (220) peak, it is clear that the lattice parameters of Pt-based bimetallic catalysts are different from each other as shown in Table 1. After fitted with Gaussian line shape, the (220) peak is used to calculate the average size of catalyst particle according to the Debye–Scherrer formula as follows (Eq. 1), where the L is average particle size, $\lambda_{K\alpha 1}$ is the wavelength of X-ray, θ_B is the angle of (220) peak, and $B_{(2\theta)}$ is the full width at half-maximum (FWHM) of the peak broadening in radians. The average particle sizes of different catalyst samples calculated for XRD results are listed in Table 1, in which the angles of (220) peaks and the FWHM are also included.

$$L = \frac{0.9\lambda_{K\alpha 1}}{B_{(2\theta)}\cos\theta_B} \quad (1)$$

The fcc lattice parameters for single-phase Pt-based catalyst in the present work were evaluated from the angular position of the (220) peaks, and the calculated values are also listed in Table 1. It is clear that the addition of Sn to the Pt extends the fcc lattice parameters, and lattice parameters of PtSn catalyst increases with the Sn content. The addition of Ru results in the decrease of Pt fcc lattice parameter compared to that of pure Pt. The differences of the lattice parameters of PtSn samples and PtRu sample indicate that the interaction between Pt and Sn is contrary to that between Pt and Ru [11]. The inference is further verified by the following results. The fcc lattice parameters of PtSn catalyst decrease again when PtSn is modified further by Ru. As it can be observed from Fig. 3, the 2θ angle of (220) peak for Pt_4Sn_1/C is shifted from 67.17° to 67.29° for $Pt_4Sn_1Ru_1$/C because of the addition of Ru. The same phenomena of 2θ angle returning also take place in other carbon-supported PtSn catalysts after Ru addition, and their comparisons are shown in Fig. 3. Here only exhibits of the line shape fitted with Gaussian and the raw data of different (220) peaks are not shown in order to preserve the figure orderly. Although shifted to higher 2θ angle after modified by Ru addition, (220) peaks of all PtSn-based catalysts appear at lower positions than that of Pt/C and Pt_1Ru_1/C.

The sizes of the nanoparticles of different Pt-based catalysts were also investigated by TEM. Most of metal

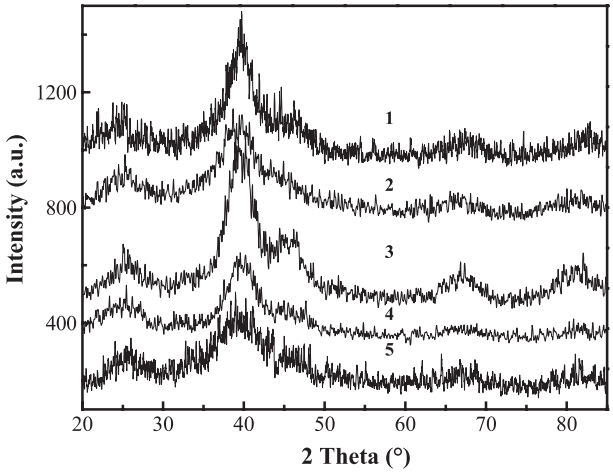

Fig. 2. XRD of PtRuSn/C with different atomic ratios 1: $Pt_2Ru_2Sn_1$/C; 2: $Pt_1Ru_1Sn_1$/C; 3: $Pt_3Ru_1Sn_2$/C; 4: $Pt_4Ru_1Sn_1$/C; 5: $Pt_2Ru_1Sn_1$/C.

Table 1
Results of XRD and TEM of carbon-supported Pt and Pt-bimetallic catalysts

Catalyst		$2\theta_{max}$ (°)	Lattice Parameter (Å)	$B_{(2\theta)}$ (mrad)	Mean particle size (nm)	
					XRD	TEM
Pt/C		67.62	3.9156	64.18	2.6	2.7
Pt_1Ru_1/C		68.26	3.8830	93.06	1.8	1.9
PtSn/C (Pt/Sn=)	1:1	66.24	3.9873	78.88	2.1	2.3
	3:2	66.50	3.9735	87.26	1.9	2.2
	2:1	66.82	3.9562	63.88	2.6	3.0
	3:1	66.89	3.9530	87.47	1.9	2.2
	4:1	67.17	3.9383	87.60	1.9	2.3

particles for every catalyst sample were less than 6 nm, and the nanoparticles show homogeneous dispersion with similar particle sizes. Most of particles were spherical in shape, and no agglomerations were observed. The particle size was approximately 1.5–3.5 nm with a very narrow size distribution, which was in good agreement with the XRD data. The TEM results of bimetallic samples are also shown in Table 1. Both XRD and TEM results indicate that all catalysts investigated in present work have similar nanoparticle sizes and the method is suitable to prepare nanometer catalysts with higher metal loading.

3.2. Single-cell test results

Carbon-supported Pt, PtRu and PtSn catalysts were used as anode catalyst and evaluated in the single-cell tests for DEFCs. The single cells with different anode catalysts show different steady-state polarization curve, as exhibited in Fig. 4. As one can observe from Fig. 4, when Pt/C is used as anode catalyst, the single cell gives a poor performance, even though the metal loading is as high as 2.0 mgPt/cm^2 on anode side. The open-circuit potential is as low as 0.55 V at 90°C, which is far from the standard electromotive force of 1.145 V [5]. The great difference between the open-circuit potential and standard electromotive force is mainly attributed to lower anode catalytic activity and ethanol crossover from anode to cathode. It is noteworthy that ethanol crossover in the present work is identical because of the same electrolyte and MEAs preparation procedures adopted in all single-cell tests. A significant potential drop of about 0.28 V, more than half of the open-circuit potential, is observed when a current density of 30 mA/cm^2 passes through this fuel cell, and the

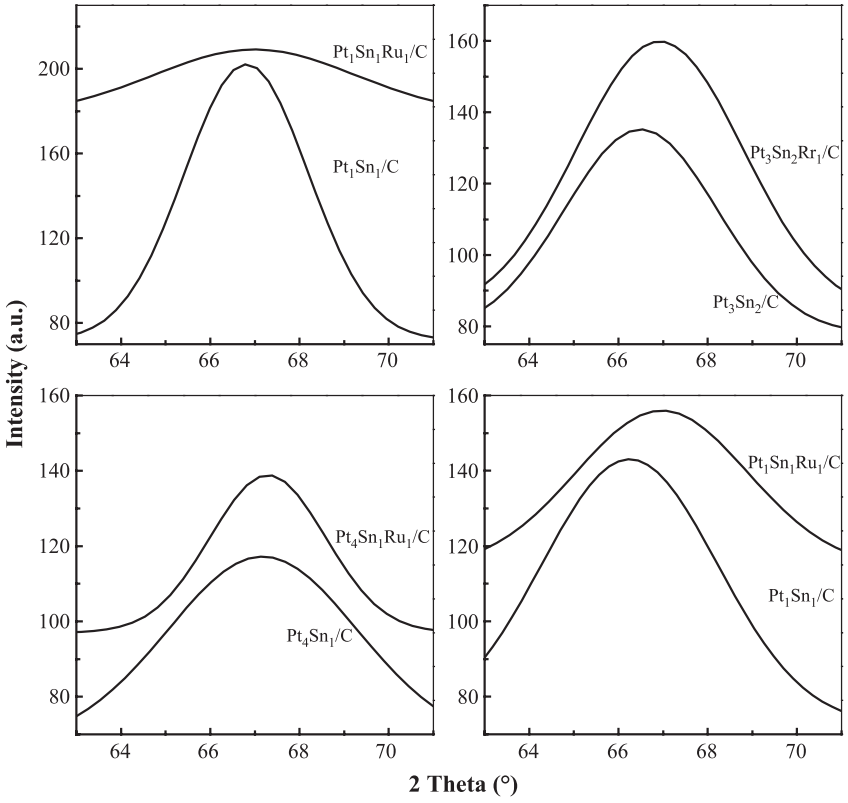

Fig. 3. Comparison of (220) peaks of PtSn/C catalyst and PtSnRn/C catalysts.

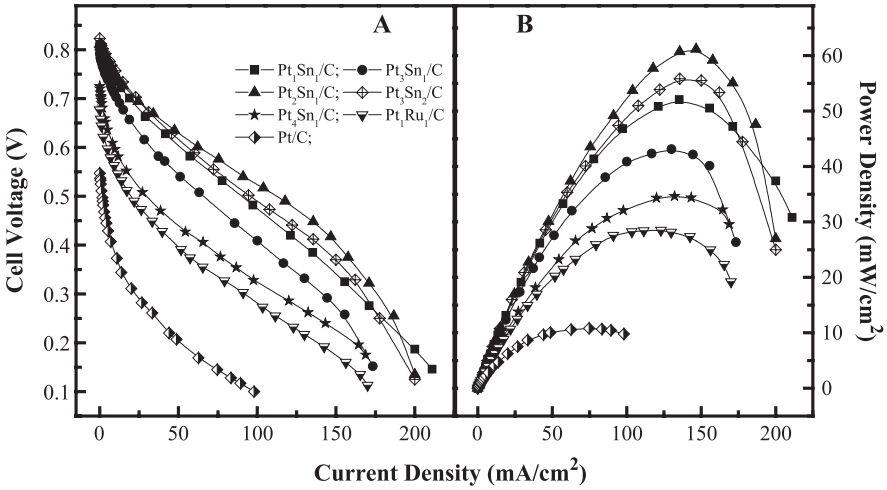

Fig. 4. Comparison of the performance of single cell with different carbon supported Pt-based catalysts as anode catalysts at 90 °C (A is the cell voltage–current density curves and B is the power density–current density curves.). Nafion®-115 membrane is electrolyte. Anode metal loading is 1.33 mgPt/cm^2. Cathode: 1.0 mgPt/cm^2. Ethanol concentration and flow rate: 1M and 1.0 ml/min. P_{O2}: 0.2 MPa.

corresponding power density at 30 mA/cm^2 was only 8.1 mW/cm^2. This behavior indicates a strong activation control for ethanol electro-oxidation at low current densities. The maximum power density of the single cell with Pt/C as anode is less than 11.0 mW/cm^2, namely 10.8 mW/cm^2 at 75 mA/cm^2.

It is obvious that the additions of Ru to Pt enhance the catalytic activity to ethanol electro-oxidation [12], and consequently greatly improve the single fuel cell performance. As observed from Fig. 4, the open-circuit voltage of single ethanol cell increases to 0.68 V when Pt_1Ru_1/C replaces the Pt/C at anode side, in which Pt accounts for 2/3 of the total metal loading of 2.0 mg/cm^2. The voltage of single cell is 0.46 V at a current density of 30 mA/cm^2, and the potential drop from open-circuit voltage is 0.22 V, about 1/3 of the open-circuit voltage. The corresponding power density is 13.8 mW/cm^2 at 30 mA/cm^2. At current density higher than 30 mA/cm^2, there is a linear variation of voltage vs. current density, which is mainly affected by the internal resistance of this fuel cell. There is no obvious mass-transfer polarization those are common in DMFCs. A peak power density of about 28.0 mW/cm^2, which is about 1/5 of the maximum power density obtained in DMFCs with the same anode catalysts and at the same operation temperature [13], is obtained in the corresponding current density range from 110 to 130 mA/cm^2.

It is also observed from Fig. 4, as Pt_1Sn_1/C, in which Ru of Pt_1Ru_1/C is replaced by equal atomic amount of Sn, is employed as anode catalyst in single direct ethanol fuel cell, the open-circuit voltage of single cell rises to 0.81 V compared to 0.68 V of single cell with Pt_1Ru_1/C. There is a small potential drop of about 0.15 V from the open-circuit voltage when the current density increases from 0 to 30 mA/cm^2 in the activation control region. The cell voltage with Pt_1Sn_1/C at 30 mA/cm^2 is close to that with Pt_1Ru_1/C, which indicates Pt_1Sn_1/C is more active to ethanol electro-oxidation than Pt_1Ru_1/C. The linear voltage drop vs. current density also appears in the single cell adopting Pt_1Sn_1/C as anode catalyst. Even at 60 mA/cm^2, the cell voltage is still as high as 0.58 V, and the corresponding power density is 34.8 mW/cm^2, which exceeds the peak power density of the single cell employing Pt_1Ru_1/C as anode. The cell voltage decreases to 0.5 V as the current density increases to 90 mA/cm^2, bringing about a power density of 45.0 mW/cm^2. This single cell gives a peak power density of 52.0 mW/cm^2, nearly twice of the single cell with Pt_1Ru_1/C.

In Fig. 4, the performances of single cells with Pt_4Sn_1/C and Pt_3Sn_1/C, are inferior to the cell employing Pt_1Sn_1/C, but still superior to those employing Pt/C and Pt_1Ru_1/C. The electrode of both single cells contain the same platinum loading and different tin loading, which is much cheaper than platinum. It is found that the open-circuit voltages of all single cells with PtSn as anode catalyst are over 0.7 V, higher than that with Pt_1Ru_1/C. For the cell with Pt_4Sn_1/C, the potential drops from 0.73 to 0.5 V when the current density increases from 0 to 30 mA/cm^2, and the corresponding power density is 15.0 mW/cm^2. Then, the cell voltage descends slowly from 0.5 to 0.42 V as the current density increases from 30 to 60 mA/cm^2. The peak power density of this cell with Pt_4Sn_1/C is 34.6 mW/cm^2, appearing at 132 mA/cm^2. When Pt_3Sn_1/C is employed as anode catalyst, namely the Sn loading increases while Pt loading is still kept the same, the cell performance is improved. Compared to the cell with Pt_4Sn_1/C, the open-circuit voltage of the cell with Pt_3Sn_1/C approaches 0.79 V. The cell voltage at 30 mA/cm^2 is also elevated to 0.61 V. The cell voltage at 60 mA/cm^2 is 0.52 V giving a corresponding power density of 31.2 mW/cm^2, which is close to the peak power density of the cell with Pt_4Sn_1/C. The power density curve arrives its peak (43.0 mW/cm^2) at 130 m A/cm^2 in the process of mild descend of cell voltage vs. current density curve. The open-

circuit voltage of the cell adopting Pt_2Sn_1/C is 0.81 V, as high as the cell with Pt_1Sn_1/C. And the cell voltage loses about 0.13 V as the current density increases from 0 to 30 mA/cm^2, and the corresponding power density at this point is 20.4 mW/cm^2. The cell voltage decreases quite slowly from 0.68 V (at 30 mA/cm^2) to 0.61 V as the current density increases to 60 mA/cm^2. The peak power density of this cell is over 60 mW/cm^2 at the current density of 146 mA/cm^2, after which, the there is a decrement of cell voltage as the current density increases. When the Sn atomic content increases to 40%, namely Pt_3Sn_2/C is employed as anode catalyst for direct ethanol fuel cell, the open-circuit voltage increases to 0.82 V. The cell voltages are 0.68 and 0.59 V at the current density point of 30 and 60 mA/cm^2, respectively. The peak powder density is 55.8 mW/cm^2 at the corresponding current density of 135.6 mA/cm^2.

The performances of the single cells with different PtSn catalysts are summarized in Fig. 5, in which every curve denotes the relation between the Sn atomic content of different PtSn anode catalysts and power density of the corresponding single cells at a given current density point such as 30, 60, 90 mA/cm^2. It is clear that there is a power density peak in every performance curve at the same Sn atomic content of about 33%, and the corresponding Pt/Sn atomic ratio is 2. From the practical point of view, the single-cell test is the final evaluation criterion for novel electrocatalysts and electrolyte, although there are so many factors influencing the performance of single cell such as activities and conductivities of electrocatalysts [14]. In the present work, anode catalyst is the one and only variable and other factors are defined such as cathode catalyst, electrolyte and MEA preparation parameters. Therefore, the single-cell performances with different anode catalysts embody the activities of anode catalysts to a certain extent. Catalyst surface structure, metallic particle size, the interaction between active components and other factors affect the activity of anode catalysts. At present, the metallic particle size effect on the ethanol electro-oxidation is not excluded although it was not verified. On the other hand, all the catalysts synthesized with the same method have similar particle size, thus the effects of particle size are similar if there is size effect. Furthermore, Sn or its oxides [15], as well as Ru, can supply surface oxygen-containing species for the oxidative removal of CO-like species strongly adsorbed on adjacent Pt active site, which is the so-called bifunctional mechanism [16]. Thus, the additions of Ru or Sn to Pt enhance the ethanol electro-oxidation, and consequently improve the fuel cell performance compared to that with pure Pt as anode catalyst. The obvious difference among these catalysts is the change in lattice parameters characterized from the XRD results as mentioned above. Ethanol electro-oxidation is alien to that of methanol in that the former is involved in the cleavage of C−C bond besides the oxidative removal of the poisoning species such as CO_{ads}. A primary prediction is that the extended lattice parameter is propitious to break the C−C bond, and the sufficient cleavage of C−C bond improves the fuel utilization and sequentially the performance of fuel cell. It is found that most of Sn are in oxidized state from the XPS results, and the catalyst conductivity decreases as the Sn content increases, which counteracts to a certain extent the promotion effect of Sn on ethanol electro-oxidation. On the other hand, Pt active sites of catalysts with high Sn content will be blocked partly by surface Sn or its oxides, which will inhibit ethanol adsorption when ethanol adsorption is the rate-determining step at high current density or higher temperatures. These opposite effects determine the optimum content of Sn. According to these standard and from the present results, it is demonstrated that Pt_2Sn_1/C is the best suitable anode catalyst for direct ethanol fuel cells operated at 90 °C in the present work.

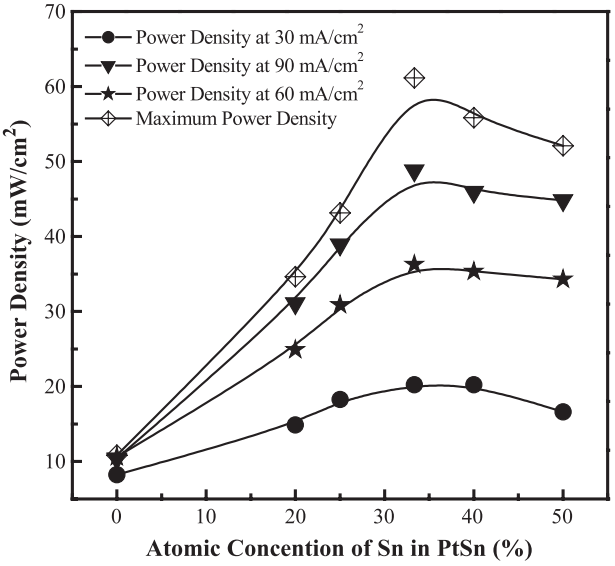

Fig. 5. The relation between the power densities of single cells at 90 °C and Sn content in different carbon supported PtSn catalysts. Nafion®-115 membrane is electrolyte. Anode metal loading is 1.33 mgPt/cm^2. Cathode: 1.0 mgPt/cm^2. Ethanol concentration and flow rate: 1M and 1.0 ml/min. P_{O2}: 0.2 MPa.

Acknowledgements

Authors would like to thank the "Greece-China Joint Research and Technology Programme 2003–2005" for funding. We also thank the financial support of National Natural Science Foundation of China (Grant No.: 20173060).

References

[1] S.C. Thomas, X.M. Ren, S. Gottsfeld, P. Zelenay, Electrochim. Acta 47 (2002) 3741.
[2] H. Dohle, H. Schmitz, T. Bewer, J. Mergel, D. Stolten, J. Power Source 106 (2002) 313.
[3] C. Rice, S. Ha, R.I. Masel, P. Waszczuk, et al., J. Power Sources 111 (2002) 83.

[4] J.T. Wang, S. Wasmus, R.F. Savinell, J. Electrochem. Soc. 142 (1995) 4218.
[5] C. Lamy, E.M. Belgsir, J.M. Leger, J. Appl. Electrochem. 31 (2001) 799.
[6] A.S. Aricò, P. Cretì, P.L. Antonucci, et al., Electrochem. Solid-State Lett. 1 (1998) 66.
[7] H. Hitmai, E.M. Belgsir, J.M. Léger, C. Lamy, R.O. Lezna, Electrochim. Acta 39 (1994) 407.
[8] N. Fujiwara, K.A. Friedrich, U. Stimming, J. Electroanal. Chem. 472 (1999) 120.
[9] W.J. Zhou, Z.H. Zhou, S.Q. Song, W.Z. Li et al., Appl. Cataly. B (in press).
[10] V. Radmilović, H.A. Gasteiger, P.N. Ross, J. Catal. 154 (1995) 98.
[11] A.K. Shukla, A.S. Aricò, K.M. El-Lhatib, et al., Appl. Surf. Sci. 137 (1999) 20.
[12] A.S. Arico, A.K. Shukla, K.M. El-Khatib, et al., J. Appl. Electrochem. 29 (1999) 671.
[13] W. Zhou, W. Li, Z. Zhou, S. Song, Z. Wei, G. Sun, Q. Xin. Chem. J. China. Univ., in press.
[14] D.L. Boxall, G.A. Deluga, E.A. Kenik, et al., Chem. Mater. 13 (2001) 891.
[15] T. Frelink, W. Visscher, J.A.R. VanVeen, Surf. Sci. 335 (1995) 353.
[16] B. Gurau, R. Viswanathan, R. Liu, T.J. Lafrenz, et al., J. Phys. Chem., B 102 (1998) 9997.